

# A method for measurement of the top quark mass using the mean decay length of $b$ hadrons in $t\bar{t}$ events.

C. S. Hill, J. R. Incandela, and J. M. Lamb

*The University of California Santa Barbara*

(Dated: July 26, 2017)

## Abstract

We present a new method for the experimental determination of the top quark mass that is based upon the mean distance of travel of  $b$  hadrons in top quark events. The dominant systematic uncertainties of this method are not correlated with those of other methods, but a large number of events is required to achieve small statistical uncertainty. Large  $t\bar{t}$  event samples are expected from Run II of the Fermilab Tevatron and the CERN Large Hadron Collider (LHC). We show that by the end of Run II, a single experiment at the Tevatron could achieve a top quark mass uncertainty of  $\sim 5 \text{ GeV}/c^2$  by this method alone. At the CERN LHC, this method could be comparable to all others methods, which are expected to achieve an uncertainty of  $\sim 1.5 \text{ GeV}/c^2$  per experiment. This new method would provide a useful cross-check to other methods, and could be combined with them to obtain a substantially reduced overall uncertainty.

PACS numbers: 12.15.Ff,13.25.Hw,14.65.Ha,14.80.Bn

## I. INTRODUCTION

There are important reasons for measuring the properties of top quarks [1]. If there are new strong interactions at the TeV scale, the top quark often plays a central role in the corresponding theories. The large top quark mass is important in extensions of the standard model, particularly when mass dependent couplings are considered. New particles are experimentally constrained to be heavier than other fermions but could be lighter than the top quark. Careful studies of top quark decay products could therefore be fruitful. Indeed the large top quark mass and its approximately unit value Yukawa coupling to the Higgs particle are often cited as a hint that the top quark has a special place in the greater scheme of things [2].

The mass of the top quark,  $m_t$ , is an important Standard Model parameter that enters quadratically into higher order corrections to the  $W$  mass,  $M_W$ , along with the Standard Model Higgs mass,  $M_H$ , which enters logarithmically. Precise values of both  $M_W$  and  $m_t$  can thus be used to constrain the Standard Model expectation for  $M_H$  [3]. Prior to observation of the Higgs, this information could be used to guide experimental searches. After the Higgs has been observed, it can be used as an interesting consistency check. If the observed Higgs mass were to be inconsistent with the prediction obtained from precision measurements of  $m_t$  and  $M_W$ , this would indicate that nature is not governed by a Standard Model Higgs sector. For these reasons it is essential to measure  $m_t$  and  $M_W$  to the best possible precision.

In this article we present a new method for the measurement of the top quark mass that is based upon the observation that the mass is correlated in a relatively strong and unambiguous way with the mean distance of travel of the  $b$  hadrons [4] formed from the  $b$  quarks produced in top quark decays [5]. The dominant systematic uncertainties of this method are associated with those factors that influence the mean  $b$  hadron decay length, such as  $b$  quark fragmentation,  $b$  hadron lifetimes, and our ability to understand and to accurately model the momenta of the top quarks and their decay products. It will be seen that jet energy scales, the dominant systematic uncertainties in other methods, result in a relatively small contribution to the uncertainty in the mean  $b$  hadron decay length. As a result, this technique can provide an independent measurement that can be used to cross-check, or be combined with, results from other methods to yield a more robust, accurate, and precise final value for  $m_t$ .

The top quark was first observed nearly a decade ago in collisions of protons with anti-protons at a center of mass energy of  $\sqrt{s} = 1.8$  TeV during Run I of the Fermilab Tevatron by the CDF and D0 experiments [6, 7]. Using the relatively small Run I  $t\bar{t}$  event samples, and combining the results of both experiments, the mass of the top quark was determined to be [8]:

$$m_t = 178.0 \pm 2.7 \text{ (stat)} \pm 3.3 \text{ (sys)} \text{ GeV}/c^2 \quad (1)$$

This result was the fruit of a very substantial effort by large teams of physicists on both experiments that benefited from an innovative improvement in methodology [9]. After Run I, there were substantial upgrades to the Fermilab accelerator complex, including an increase of beam energies to  $\sqrt{s} = 1.96$  TeV, and to the CDF and D0 experiments. Tevatron Run II began in 2001 and is scheduled to last until slightly beyond the startup of the CERN Large Hadron Collider (LHC). In this period, Tevatron experiments could collect top quark samples that are almost two orders of magnitude larger than those of Run I. These will enable the CDF and D0 experiments to significantly improve their measurements of  $m_t$ . Each experiment currently expects to achieve an overall uncertainty of roughly 2-3  $\text{GeV}/c^2$  [10].

The CERN LHC will supersede the Tevatron as the world's highest energy accelerator when it begins operation later this decade. The LHC will collide protons with protons at a center of mass energy of  $\sqrt{s} = 14$  TeV. The 7-fold increase in energy relative to the Tevatron means that the dominant  $t\bar{t}$  production mechanism will change from quark-anti-quark annihilation to gluon fusion. As a result, the  $t\bar{t}$  production cross-section rises from a calculated value of 6.7 pb [11, 12] at the Tevatron, to 833 pb [11] at the LHC. The LHC will also operate at higher luminosity than the Tevatron. The net effect is that the LHC will produce  $\sim 8\text{M}$   $t\bar{t}$  events per year [13] at its initial operating luminosity of  $10^{33} \text{ cm}^{-2} \text{ sec}^{-1}$ . This number will rise by an order of magnitude for high luminosity operation. Availability of such large top quark samples will mean that all measurement techniques will rapidly become limited by systematic uncertainties, which are expected to be  $\sim 1.5 \text{ GeV}/c^2$ . This will also be true for the extraction of the top quark mass from the mean  $b$  hadron decay length.

In this article we present estimates for the potential top quark mass resolution of this new method at both the Tevatron and the LHC. In Section II we describe in detail the aspects of the method that are common to its application at both accelerators. In particular, we discuss the important sources of uncertainty and how they are estimated. The approaches taken for the Tevatron and LHC are not identical, mainly due to the fact that Tevatron measurements

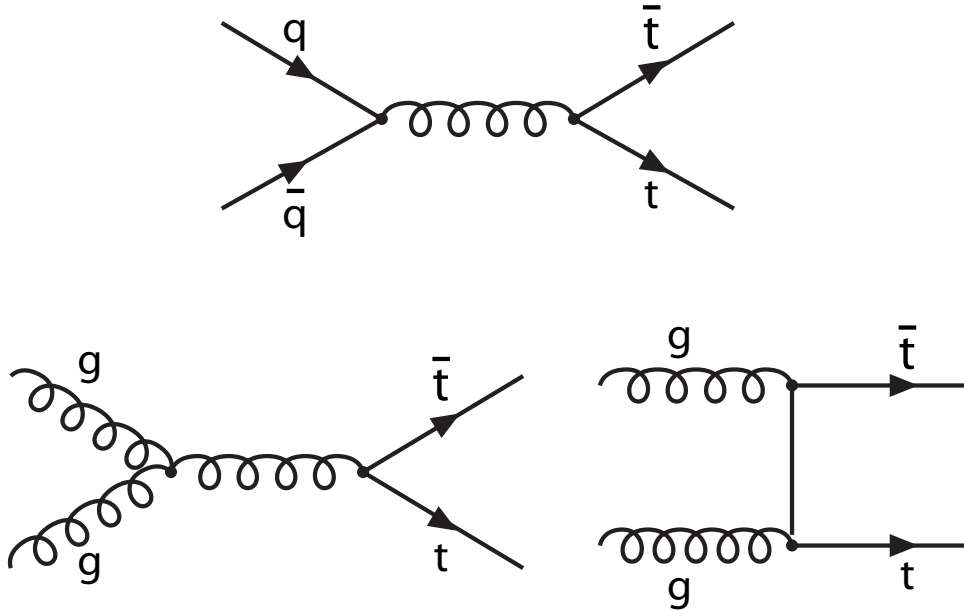


FIG. 1: Feynman diagrams showing the leading order  $t\bar{t}$  production mechanisms.

will be statistically limited, even for the most optimistic projections of integrated luminosity. On the other hand, the large  $t\bar{t}$  event rates at the LHC allow one to quickly achieve statistical uncertainties below  $1 \text{ GeV}/c^2$ , even in the most pessimistic operating scenarios. This allows us to define event selection criteria that minimize uncertainties. Descriptions of the event selection and several other aspects of our studies that are unique to a given accelerator environment are postponed until sections III A and III B, where we also report the results of our studies for the Tevatron and LHC, respectively. It will be seen that variations in the estimated uncertainties in the two accelerator environments can be traced, among other things, to a difference in the dominant  $t\bar{t}$  production mechanism.

Our basic approach is to use Monte Carlo programs [14, 15] currently in use by Tevatron and LHC experimental groups to generate  $t\bar{t}$  events at the appropriate beam energies. We do not perform full simulations of any of the Tevatron or LHC experiments. Rather, we include the effects of imperfect pattern recognition and detector resolution by smearing Monte Carlo generated decay lengths to obtain a reasonable match to distributions seen in collider data and full detector simulations. In fact, we find that detector modeling has relatively little effect on the estimated uncertainties in  $m_t$  for this method. As described in section III A, for the Tevatron study we consider backgrounds such as  $Wb\bar{b}$  and misidenti-

fication of light quark jets as  $b$  jets (“mistags”) in  $W + \text{jets}$  and multi-jet events. For the LHC, as described in section III B, we choose an event selection that reduces backgrounds to negligible levels. In addition, a jet veto is used to suppress events containing significant QCD radiation, thereby minimizing the uncertainties associated with Monte Carlo modeling of these processes. In section IV we discuss ways in which improvements are likely or possible. Finally, we summarize our results and present our conclusions in section V.

The results presented below, while representative of what one could reasonably expect to observe, include values for mean  $b$  decay lengths in  $t\bar{t}$  events that are not intended to exactly predict those that one would extract experimentally. For example, the kinematic criteria used in event selection, as well as detector specific effects, will cause variations in the observed mean  $b$  hadron decay length for a given top quark mass. Nevertheless, we have estimated uncertainties carefully and we have verified that they are robust to variations in the modeling of detector effects. Our projections for the uncertainties on the top quark mass are thus expected to be accurate predictions of what can be expected at the Tevatron and LHC in coming years.

## II. THE METHOD

The Fermilab Tevatron currently collides protons with anti-protons at  $\sqrt{s} = 1.96$  TeV. At this energy, the dominant  $t\bar{t}$  production mechanism is  $q\bar{q}$  annihilation. Valence quarks carry  $\sim 15\%$  of the proton momentum on average, corresponding to a constituent collision energy of  $\sqrt{\hat{s}} \sim 300$  GeV. The  $t\bar{t}$  system is therefore produced near threshold. The  $t\bar{t}$  pair can have transverse momentum as a result of initial state radiation. This is typically below 100 GeV, corresponding to a relativistic boost that is very near to unity:  $\gamma - 1 \leq 0.04$ . In general, there is little energy available to provide the individual top quarks with large transverse momenta. In spite of a 7-fold energy increase to  $\sqrt{s} = 14$  TeV,  $t\bar{t}$  events at the LHC will be similar to those at the Tevatron in many ways. This is mainly due to the fact that the dominant production mechanism at the LHC is gluon fusion ( $gg \rightarrow t\bar{t}$ ). As a result,  $t\bar{t}$  pairs are once again produced near mass threshold ( $\sqrt{\hat{s}} \sim 350\text{-}400$  GeV), albeit with a more substantial fraction appearing at higher  $\sqrt{\hat{s}}$ . Fig. 2 shows distributions of  $\sqrt{\hat{s}}$  underlying  $t\bar{t}$  production at the Tevatron and LHC as obtained with the PYTHIA Monte Carlo [14].

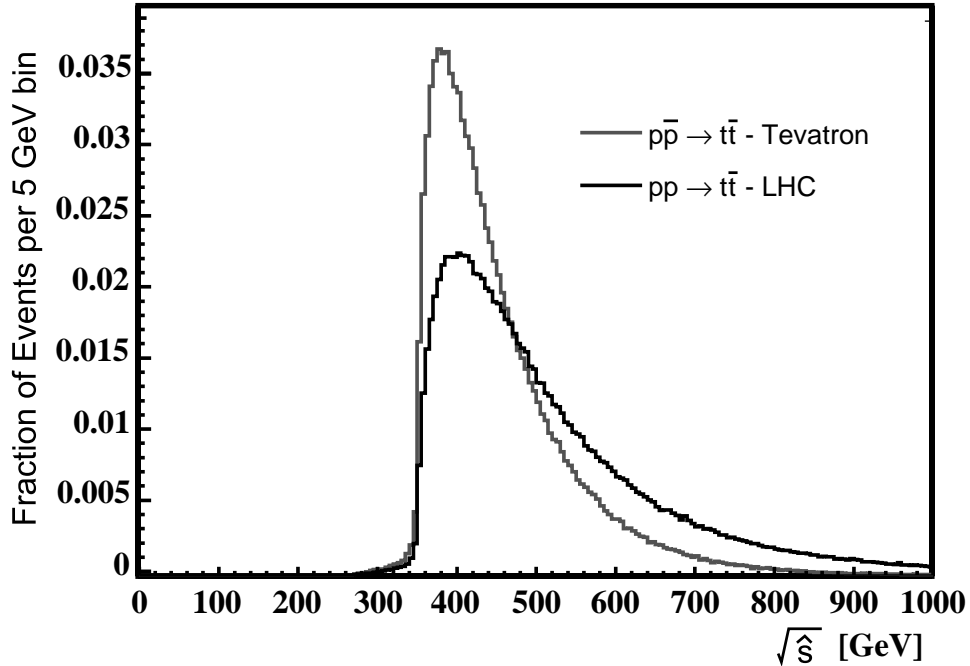


FIG. 2: PYTHIA Monte Carlo comparison of the distributions of constituent center of mass energies ( $\sqrt{\hat{s}}$ ) underlying  $t\bar{t}$  production at the Tevatron and LHC for  $m_t = 175 \text{ GeV}/c^2$ .

In the Standard Model, the top quark decay proceeds almost uniquely as  $t \rightarrow Wb$ . In the rest frame of the top quark, the  $W$  and  $b$  daughters have equal and opposite momenta of magnitude:

$$p = \frac{m_t c}{2} \sqrt{(1 - ((M_W^2 - m_b^2)/m_t^2))^2 - 4(M_W m_b/m_t^2)^2} \quad (2)$$

Thus,  $p/c \sim 0.4 m_t$  for large  $m_t$ , and the relativistic boost of the  $b$  quark is substantial,  $\gamma_b \sim 0.4 \times (m_t/m_b)$ . As a consequence, the  $b$  quark momentum is potentially a sensitive gauge of the top quark mass. One could use the correlation of the  $b$  jet energy to the top quark mass directly. The drawback of this approach, however, is that it depends upon the  $b$  jet energy measurement which suffers from a jet energy scale uncertainty like other methods.

As an alternative, consider the mean  $b$  hadron decay length,  $\langle L \rangle$ , which is also correlated with the  $b$  momentum. For a  $b$  hadron of momentum  $p$ , mass  $m_b$ , and proper life time  $\tau_o$  one obtains:

$$\langle L \rangle = c\tau_o\beta\gamma = \tau_o \frac{p}{m_b} \quad (3)$$

This expression provides the dependence on the energy since  $E = \sqrt{(pc)^2 - (m_b c^2)^2} \sim pc$ . The key point is that  $\langle L \rangle$  can be found directly without measuring  $E$ . It is simply the average measured distance from the primary interaction vertex to the  $b$  hadron decay vertex. It thus depends upon charged particle track reconstruction as opposed to jet energy reconstruction. Tracks are formed by fitting “hits” to helical trajectories. The hits are measurement points on charged particle trajectories that are typically obtained with a precision of 5-50  $\mu\text{m}$  in semiconductor tracking detectors, such as silicon micro-strips or pixels.

In practice, we use the average of the transverse decay length,  $L_{xy} = L|\sin\theta|$ , where  $\theta$  is the angle of the  $b$  hadron flight path with respect to the beam axis. This is necessitated by the fact that the net longitudinal momentum of the  $t\bar{t}$  pair is not known in hadron collisions. The partons themselves have broad momentum distributions within the proton or anti-proton. The sum over the transverse momenta of all objects in the event must however be zero. In terms of the transverse energy  $E_T \equiv E \sin\theta$ , and mass of the  $b$  hadron, we have:

$$\langle L_{xy} \rangle = c\tau_o \sqrt{\left(\frac{\langle E_T \rangle}{m_b c^2}\right)^2 - 1} \quad (4)$$

Equations 2 and 4 provide a simple basis for understanding the correlation between the mean  $b$  hadron transverse decay length and the top quark mass. There are, however, a large number of additional factors that influence this correlation, and therefore need to be understood and taken into account. These factors can be categorized as follows:

- Factors that affect the momentum of the top quark:
  - Initial state QCD radiation from colliding partons.
  - Final state QCD radiation from top quarks.
  - Interference of final and initial state radiation.
  - Parton density functions of the beam particles.
  - Spin correlations.
- Factors that affect the  $b$  hadron momentum and decay length:

- Fraction of  $b$  quark momentum carried by the  $b$  hadron, (i.e. fragmentation).
  - Radiation from the  $b$  quark.
  - Relative proportions of  $b$  hadron species.
  - Lifetimes of the  $b$  hadron species.
  - Modeling  $b$  hadron decays.
  - $b$  hadron identification and vertexing efficiency (“ $b$  tagging”).
  - Dependence of  $b$  tagging on  $b$  jet momentum.
- Background events mistakenly identified as  $t\bar{t}$ .
  - Accidental  $b$  tagging of light quark jets (“mistags”).
  - Additional factors:
    - Kinematic selection of events.
    - Tracking efficiency, purity, and precision.
    - Multiple interactions in a single beam-beam crossing.

#### **A. Basic procedure for determination of $m_t$ and its uncertainties.**

We now give a broad overview of the basic procedures that were used in our studies, followed by more detailed presentations of some of the key steps. As mentioned above, the specific implementations of this method at the Tevatron and LHC differ in some respects. Details that are only pertinent to a specific accelerator environment are deferred to sections III A and III B, where we describe the results of our Tevatron and LHC studies, respectively.

##### *1. Overview*

The procedure we follow for our studies is relatively straightforward. We create “default”  $t\bar{t}$  samples using the PYTHIA Monte Carlo. We do not perform a full detector simulation of the events. We apply event selection criteria directly to the Monte Carlo generated transverse momenta of electrons, muons, and jets in the events. A missing transverse energy, ( $\cancel{E}_T$ )



requirement is applied to the transverse component of the vector sum of the 4-vectors of all neutrinos in the event.

For a given choice of  $m_t$ , we generate a large number of events. Prior to a determination of  $L_{xy}$  for a  $b$  hadron decay, we require there to be an adequate number of daughter particles with significant impact parameters relative to the primary vertex that can be used to form a secondary decay vertex. The impact parameters of these particles are smeared according to relevant experimental resolutions. The particles must pass typical selection criteria. The event selection criteria and experimental resolutions, which are typical of Tevatron and LHC experimental studies, are detailed in Sections III A and III B. If it is determined that the vertex could potentially be observed experimentally, then the associated  $L_{xy}$  value is obtained by simply smearing the Monte Carlo generated transverse decay length of the  $b$  hadron.

This procedure is repeated for different choices of  $m_t$ . We also generate background event samples that are selected and processed in a similar manner. We combine signal and background events in the proportions expected for a given experiment and choice of event selection criteria. For each  $m_t$ , the combined signal plus background sample is used to obtain a mean value of the transverse decay length,  $\langle L_{xy} \rangle$ . These values are plotted as a function of  $m_t$  and they are fit to a polynomial in  $m_t$ , as seen in Fig. 3. For a given choice of beam energy, event selection, and  $b$  tagging algorithm, this polynomial represents our expectation for the correlation of  $m_t$  with  $\langle L_{xy} \rangle$  in  $t\bar{t}$  events. We will refer to the polynomial as the *mass estimator*.

To estimate statistical uncertainties, we form an ensemble of event samples in which the number of  $b$  hadrons from signal and background events are each randomly selected from Poisson distributions for which mean values correspond to the expectations for a specific experiment and integrated luminosity. The  $L_{xy}$  values for a given sample in the ensemble are generated using the shape of the  $L_{xy}$  distribution obtained for a given choice of signal plus background, as described above. For each sample,  $\langle L_{xy} \rangle$  is calculated and the mass estimator specific to the accelerator environment under consideration is used to obtain a corresponding value for  $m_t$ . The resulting distribution of  $m_t$  values for the full ensemble is not Gaussian, in general, since the relationship of  $m_t$  to  $\langle L_{xy} \rangle$  is not linear over large mass ranges as seen in Fig. 3. In these cases, which are relevant for small statistics experiments, one obtains asymmetrical statistical uncertainties. For high statistics experiments, only

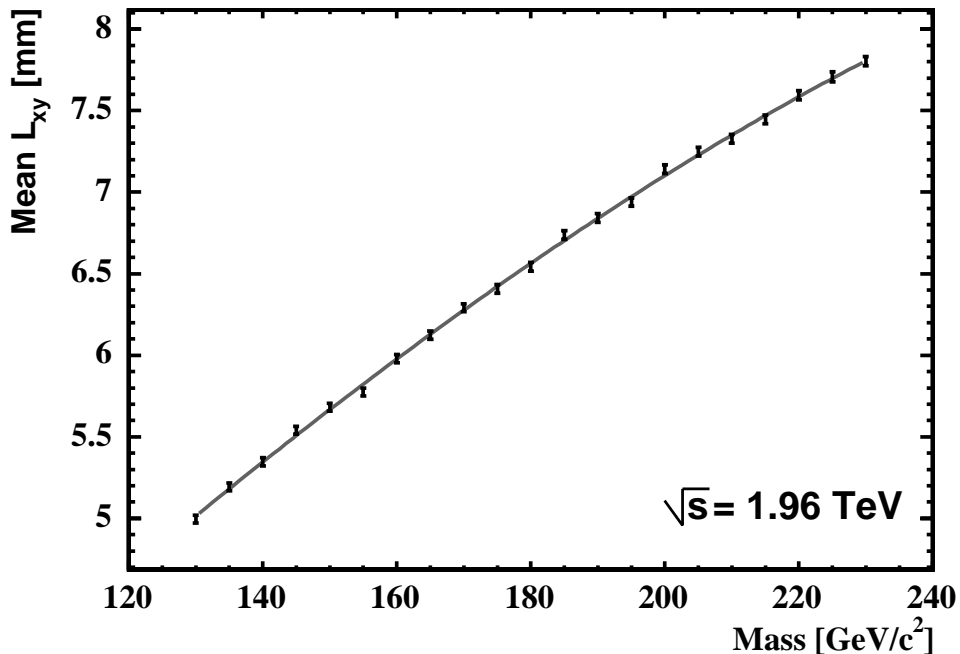


FIG. 3: An example of the correlation of  $L_{xy}$  with  $m_t$  for the default Monte Carlo and a particular choice of event selection at the Tevatron. Backgrounds, as described in the text, are also included and represent 25% of all entries. The correlation is well fit by a third degree polynomial over the full mass range as shown, and it is linear over small mass ranges. Each point represents  $\sim 50,000$   $b$  jets in Monte Carlo  $t\bar{t}$  events.

small mass ranges need to be considered and the resulting ensemble distribution for  $m_t$  is Gaussian. In these cases the standard deviation is taken to be the statistical uncertainty. The uncertainties themselves are obtained by constructing Neymann frequentist confidence intervals following the prescription described in §32.3.2.1 of reference [16].

To take into account uncertainties associated with the modeling of the underlying physics, (e.g. initial and final state radiation, and parton distribution functions), we vary the relevant Monte Carlo control parameters to produce alternative event samples from which we can again extract values of  $\langle L_{xy} \rangle$ . The original mass estimator is again used to extract values of  $m_t$ , which differ from our default values. For any particular variation, the difference with respect to the default,  $\Delta m_t$ , is our estimate of the uncertainty associated with this particular aspect of the event model. Monte Carlo parameter variations that we use are consistent with the current guidance provided by the authors of the Monte Carlos, or they

conform to current conventions used in measurements of top quark properties at the Tevatron or studies performed by detector collaborations in preparation for LHC operation.

**B.  $L_{xy}$  distributions for  $b$ ,  $c$  and light quark jets and their associated uncertainties.**

We now briefly discuss how  $L_{xy}$  is determined experimentally and the procedure used to obtain a reasonable approximation to  $L_{xy}$  using Monte Carlo generated information for  $b$  and  $c$  hadrons. We also discuss how we treat mistagged light quark jets. This is followed by a discussion of the dependence of  $b$  tagging on the  $E_T$  of the  $b$  jet. We then present how we estimate the systematic errors on  $\langle L_{xy} \rangle$  associated with the modeling of  $b$  fragmentation and the uncertainty in the average  $b$  hadron lifetime. We make the reasonable assumption that properties of  $b$  jets as measured in  $Z \rightarrow b\bar{b}$  events at LEP and SLD, and high  $p_T$   $b$  jets from direct production of  $b\bar{b}$  at the Tevatron, apply also to  $b$  jets from top quark decays. This can be justified by noting that the final stage of jet hadronization is a non-perturbative QCD process at a scale of order  $\Lambda_{QCD}$  (see for instance §4.1 of [17]).

*1. Modeling  $L_{xy}$  in  $b$ ,  $c$  and light quark jets*

The experimentally observed  $L_{xy}$  distribution for  $b$  and  $c$  jets is the result of a complicated process of particle tracking, track selection criteria, and vertex finding. While each element of this process contributes to the final shape of the  $L_{xy}$  distribution to some degree, the final outcome can be described by two main effects. Namely, a convolution of the true  $L_{xy}$  distribution with a Gaussian resolution function, and a skewing of the distribution that results from the use of tracks with significant impact parameters relative to the primary vertex. In this section we describe in more detail how these effects arise and how we treat them with a Monte Carlo simulation.

The transverse decay length is the measured distance between the point at which the primary beam particles collide, (the primary vertex), and the point at which the  $b$  hadron decays, (the secondary vertex), as projected into a plane perpendicular to the beam axis. In an actual experiment, a vertex is calculated as the intersection point of two or more charged particle tracks which have helical trajectories in the magnetic field of the tracking detector. Fig. 4 presents a schematic view of the tracking environment for a  $b$  jet from top quark

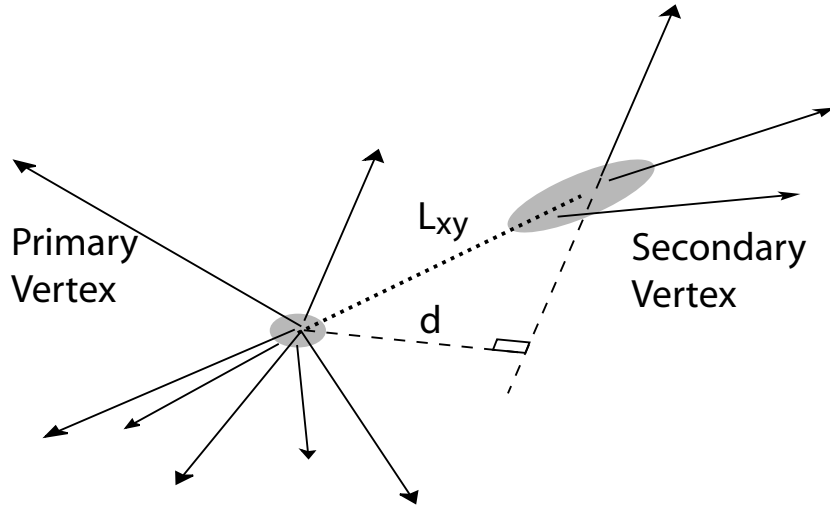


FIG. 4: Schematic representation of tracks in the vicinity of the beam-beam interaction for an event with a high energy  $b$  jet.

decay.

The primary vertex is reconstructed using all tracks that can be consistently associated with a specific, small region along the beam line. In practice, the transverse position of the primary vertex is sometimes taken from the beam line itself, as measured with many thousands of tracks, from thousands of successively recorded events, under a given set of operating conditions. The position of the  $b$  hadron decay is obtained by forming a vertex from “displaced tracks”, (i.e. tracks that have significant impact parameters relative to the beam axis). Typically a track impact parameter,  $d$ , is said to be significant when  $S_d \equiv d/\sigma_d \geq x$ , where  $\sigma_d$  is the uncertainty on  $d$ , and  $x$  is typically 2.5 or 3. The tracks are also required to be inside a cone centered on the axis of a jet, which is defined as the line joining the primary vertex to the centroid of a cluster of calorimeter towers with energies above some threshold. For high energy  $b$  jets, a cone radius  $R \equiv \sqrt{\Delta\eta^2 + \Delta\phi^2} = 0.4$  is used, where  $\Delta\eta$  and  $\Delta\phi$  are the opening angles of the cone in pseudorapidity and azimuth, respectively [18].

The sources of uncertainty in the measurement of  $L_{xy}$  include the uncertainties in the positions of the vertices due to uncertainties in the reconstructed helical track parameters, which, in turn, are affected by hit position uncertainties and detector misalignments. Other sources of mis-measurement are the inclusion of fake tracks, and the association of tracks from other vertices. Furthermore, in  $t\bar{t}$  events, the  $b$  hadrons are not fully reconstructed

and so it is often the case that the tracks used to locate the secondary decay vertex are a mixture of tracks from the  $b$  hadron decay and sequential  $c$  hadron decay. The sequential  $c$  hadron has substantial momentum and in fact travels on average 1-2 mm beyond the  $b$  hadron decay point. Use of such vertices is necessary to obtain high  $b$  tagging efficiency but requires one to loosen some vertexing criteria, such as the maximum allowed  $\chi^2$  value associated with the fit to a single vertex, but also increases the average uncertainty in  $L_{xy}$ . For the case of several displaced tracks from a single decay vertex, the uncertainty on the transverse position of the vertex is typically 100-200  $\mu\text{m}$ . This increases to  $\sim 1$  mm when the tracks used in the vertex come from both the  $b$  and sequential  $c$  hadron decays.

In our studies, we use smeared Monte Carlo generated information to reproduce the main experimental aspects of the  $L_{xy}$  distributions for  $b$  and  $c$  hadrons. For  $b$  and  $c$  jets we use the 4-vectors of daughter particles with transverse momenta above 0.5 GeV/ $c$  to calculate impact parameters with respect to the beam line. We take into account the curvature of the tracks in the magnetic field in this calculation. We then associate an uncertainty with the impact parameter of each track using parameterizations that vary with the transverse momentum of the track as:

$$\sigma_d = \sqrt{\alpha^2 + (\beta/p_t)^2} \quad (5)$$

In this expression  $\alpha$  represents the asymptotic impact parameter resolution for arbitrarily high track momenta. The second term, which depends on  $p_T$ , takes into account multiple scattering due to interactions with the detector material. The parameter  $\beta$  thus depends on both the amount and location of material in the tracker relative to where track hits are measured. The parameter  $\alpha$  includes the uncertainty associated with the primary vertex. This can be quite small when the track multiplicity is large, as is often true for  $t\bar{t}$  events. If instead one uses the position of the beam line, the relevant uncertainty is then the transverse size of the beam itself, which is  $\sim 30$   $\mu\text{m}$  at the Tevatron and will be  $\sim 15$   $\mu\text{m}$  at the LHC. In our studies we use different values for these parameters for the Tevatron and LHC. In all cases, we require that the tracks have an impact parameter significance  $S_d \geq 2.5$ . We only consider those  $b$  and  $c$  hadrons which have at least 2 significantly displaced tracks and we calculate an associated  $L_{xy}$  by shifting the true transverse decay length by a random value obtained from a Gaussian distribution centered at the origin with standard deviation  $\sigma_L = 1$  mm. This value is consistent with Monte Carlo studies of  $b$  tagging with a full

simulation of the CDF detector at the Tevatron [19]. The Gaussian smearing makes it possible for there to be negative decay lengths, (corresponding to the unphysical case of a secondary decay appearing behind the primary interaction with respect to the jet direction), while the requirement of at least two significantly displaced tracks skews the  $L_{xy}$  distribution toward positive values. The smearing and skewing just described are the most salient features of the  $L_{xy}$  distribution as it is manifested experimentally [19].

We generated large numbers of events for a range of top quark masses. We also generated large samples of background events. For each  $b$  and  $c$  jet with at least two significantly displaced tracks, we determine  $L_{xy}$  as described above. We then calculated  $\langle L_{xy} \rangle$  for combinations of top quark mass samples plus background samples and fit the results to obtain a parameterization of  $\langle L_{xy} \rangle$  versus  $m_t$ . For background events we included the  $L_{xy}$  values for mistagged light quark jets. Note that we obtain our normalizations for the signal and background jets contributing to the final  $L_{xy}$  distribution directly from recent experimental results [19], scaled to the particular integrated luminosities and  $t\bar{t}$  production rates relevant to our studies.

In light quark jets, such as those from  $W$  decay in  $t\bar{t}$  events or in backgrounds, it is possible for significantly displaced tracks to occur and lead to a false  $b$  tag. The probability that a light quark jet will be mistagged is typically less than 1%, and is generally well parameterized by collider di-jet data as a function of jet  $E_T$  and pseudorapidity [19]. Mistags are due to tracks with significant impact parameters arising from several sources. For the most part, they are tracks that originate at the primary interaction, but appear to be significantly displaced because they are on the extremes of the Gaussian resolution distribution. True displaced tracks from particles with significant lifetimes (e.g.  $K_s$ ,  $\Lambda^0$ , and photon conversions) are also sometimes incorrectly used in  $b$  tagging when the long-lived particle is not properly identified. The latter occurs when at least one of the daughter tracks is not properly reconstructed. Finally, there are fake tracks that result from pattern recognition errors such as the association of hits from two or more particles in the reconstruction of a single track. Fake tracks and tracks from long-lived particles can result in reconstructed vertex locations distributed more or less uniformly in space out to or beyond the radius of the beam pipe or first measurement layer. We model these using a flat distribution at positive  $L_{xy}$ .

Our model of the  $L_{xy}$  distribution for mistagged jets is shown in Fig. 5. The distribution

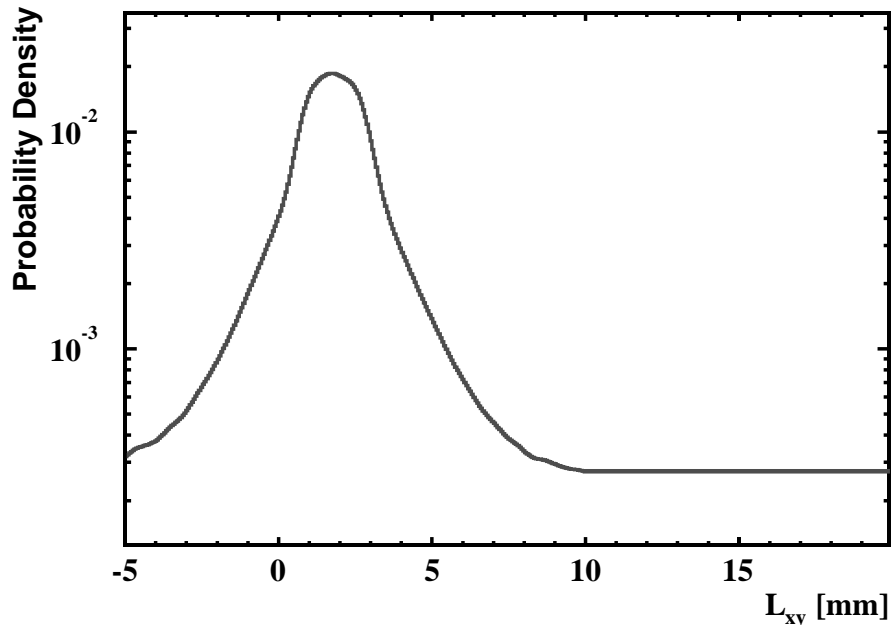


FIG. 5: The probability distribution versus  $L_{xy}$  for light quark jets with at least two significantly displaced tracks.

is consistent with measurements and full simulation of the CDF detector [19]. It is well approximated by the convolution of a Gaussian centered at  $L_{xy} \sim 2$  mm, with symmetrically rising and falling exponentials in the negative and positive  $L_{xy}$  regions, respectively, and a flat distribution at positive  $L_{xy}$ . As mentioned above, the distribution is skewed into the positive  $L_{xy}$  region as a result of the displacement significance requirement,  $S_d \geq 2.5$ , applied to the tracks.

As a check of the sensitivity of our results to our modeling of detector effects, we repeated the process described above in the absence of Gaussian smearing of  $L_{xy}$  values, and ignoring mistagged jets. We found that the parameterization of  $\langle L_{xy} \rangle$  versus  $m_t$  displayed a shift in the average transverse displacements. The slope, however, differed negligibly from our previous result. The scale shift means that the two cases yield different mass predictions for a given value of  $\langle L_{xy} \rangle$ . The invariance of the slope, however, means that the estimated systematic uncertainties are the same in both cases. The reason that the slope does not change appreciably stems from the fact that the  $L_{xy}$  distribution for any given top quark mass is approximately an exponential, while the uncertainties associated with the determination of  $L_{xy}$  are Gaussian. The mass information is contained in the slope of the distribution

which is not changed by convolution with a Gaussian. The visibility of the exponential, however, is diminished as the width of the Gaussian increases relative to the mean of the exponential. In the case of top quark decays, the mean decay length is roughly 5 mm while the  $L_{xy}$  resolution is typically 1 mm or less. Thus, our studies do not predict  $\langle L_{xy} \rangle$  exactly for a given  $m_t$ , but do provide robust predictions for uncertainties on  $m_t$ .

## 2. Tagging efficiency versus transverse energy.

The dependence of the  $b$  tagging efficiency on jet transverse energy,  $E_T$ , is influenced by many factors including the choice of the  $b$  tagging algorithm and the overall performance of the tracking system. For simplicity, we assume a dependence on jet  $E_T$  similar to that measured with  $b$  jet enriched data samples at the Tevatron [19]. Thus, we take the efficiency to rise linearly in the range  $15 \leq E_T \leq 40$  GeV from a minimum of 25% to a maximum of 40%. It then remains approximately constant for higher values of  $E_T$ . The average efficiency will affect the overall statistical uncertainty that can be achieved on  $m_t$  for a fixed integrated luminosity, while the dependence on  $E_T$  affects  $\langle L_{xy} \rangle$  and can therefore introduce a systematic uncertainty in  $m_t$ .

Studies indicate that the shape of this distribution in data is well matched by fully simulated Monte Carlo samples [19]. However, the fact that the efficiency is not constant in the low  $E_T$  region can lead to an uncertainty in  $m_t$  as a result of the jet energy scale uncertainty. This follows from the fact that event selection criteria usually involve thresholds for jets in the low  $E_T$  region in order to have good signal efficiency. The jet energy scale uncertainty thus represents a threshold uncertainty that translates into an uncertainty in the energy spectrum of  $b$  jets contributing to the  $L_{xy}$  distribution. For instance, we find that a variation in the minimum  $E_T$  threshold by an amount equal to a jet energy scale uncertainty of 10%, leads to a 1.09% systematic uncertainty in  $m_t$  in our Tevatron study.

Note, however, that the  $b$  tag efficiency need not be parameterized in terms of the jet  $E_T$ . As an alternative, the total  $p_T$  of the tracks involved in the tag, or associated with the  $b$  jet, could be used [20]. The uncertainty is then shifted from the category of calorimetry to that of tracking, analogous to the basic premise of the correlation of  $m_t$  with  $\langle L_{xy} \rangle$ . In this manner, the overall uncertainty due to the variation of tagging efficiency with the  $b$  jet  $E_T$  could be reduced substantially.



### 3. Fragmentation, $b$ hadron species, and their lifetimes

The  $b$  quarks from top quark decays pick up light quarks from the vacuum to create  $b$  mesons and baryons. The  $b$  hadron carries a fraction  $X_b$  of the initial  $b$  quark momentum, while the remainder is dispersed into the momenta of the lighter mesons created in this fragmentation process. Together with the  $b$  hadron decay products, these tracks form the  $b$  jet, which is generally well contained within a cone of radius  $R = 0.4$  in  $t\bar{t}$  events. The fragmentation function, namely the distribution of  $X_b$  values for many  $b$  jets, has been studied extensively. The most precise measurements of  $b$  fragmentation are from the study of  $Z \rightarrow b\bar{b}$  events at the LEP and SLC accelerators [21, 22, 23, 24]. For our studies, we use the single most precise measurement which comes from the OPAL experiment[21]:

$$X_b = 0.7193 \pm 0.0016 \text{ (stat)} \begin{matrix} +0.0038 \\ -0.0033 \end{matrix} \text{ (syst)}. \quad (6)$$

Fragmentation is important in the correlation of  $m_t$  with  $\langle L_{xy} \rangle$  since the momentum of the  $b$  hadron determines the relativistic boost in Eq. 4. Thus, uncertainties in the mean,  $\langle X_b \rangle$ , and in the shape of the  $X_b$  distribution could contribute systematic uncertainties to  $m_t$ . Since  $\langle L_{xy} \rangle$  is directly proportional to the average transverse momentum of the  $b$  hadrons, we determine the uncertainty associated with  $\langle X_b \rangle$  by simply varying  $\langle L_{xy} \rangle$  by a fractional amount equal to the fractional uncertainty in  $\langle X_b \rangle$ . Variations of the shape of the  $X_b$  distribution could affect  $\langle L_{xy} \rangle$ , even for a fixed  $\langle X_b \rangle$ , through the processes of event selection and  $b$  tagging. Nevertheless, since OPAL data does not strongly distinguish between a variety of theoretical models [21] for  $b$  fragmentation in  $Z$  decays, we do not associate any uncertainty with the shape of the fragmentation function.

A potential source of uncertainty associated with our treatment of  $b$  fragmentation stems from the fact that the color environment in  $t\bar{t}$  events is different from that of  $Z$  events. However, recent calculations [25] indicate a value of  $\langle X_b \rangle$  in top quark decays that is within one standard deviation of the value in Eq. 6. We have therefore assumed that the results of previous measurements can be applied to  $t\bar{t}$  events.

Taking the preceding discussion into account, we estimate a systematic uncertainty in  $m_t$  associated with  $b$  fragmentation by varying  $\langle L_{xy} \rangle$  by  $\pm 0.57\%$ , corresponding to the total uncertainty in Eq. 6.

The fragmentation process results in the production of all  $b$  hadron species. These appear

TABLE I: Fractions of  $b$  hadron species in  $Z \rightarrow b\bar{b}$  decays and their lifetimes.

| Species          | Percentage     | Lifetime          | Relative Efficiency |
|------------------|----------------|-------------------|---------------------|
| $B^0, \bar{B}^0$ | $39.7 \pm 1.0$ | $1.536 \pm 0.014$ | 1.0                 |
| $B^\pm$          | $39.7 \pm 1.0$ | $1.671 \pm 0.018$ | 1.0                 |
| $B_s, \bar{B}_s$ | $10.7 \pm 1.1$ | $1.461 \pm 0.057$ | 1.0                 |
| $b$ mesons       | $90.1 \pm 1.7$ | $1.603 \pm 0.022$ | 1.0                 |
| $b$ baryons      | $9.9 \pm 1.7$  | $1.208 \pm 0.051$ | $0.8 \pm 0.05$      |

in specific proportions, as measured by CDF and the LEP and SLD experiments [26], and with specific lifetimes [16]. As for  $b$  fragmentation, uncertainties in the  $b$  hadron lifetimes are important since  $\langle L_{xy} \rangle$  depends on them directly. To take this into account in our studies, we use the current uncertainty on the inclusive  $b$  hadron lifetime [17]:

$$\tau_b = 1.574 \pm 0.008 \times 10^{-12} \text{ sec} \quad (7)$$

This corresponds to a 0.51% variation in  $\langle L_{xy} \rangle$  if all types of  $b$  hadrons are tracked and vertexed with equal efficiency. If this is not the case, then the variation may need to be amended and an uncertainty must be introduced in association with the modeling of  $b$  hadron decays.

The current values and uncertainties for the proportions and lifetimes of the various  $b$  hadron species are summarized in Table I. For Monte Carlo  $t\bar{t}$  events with full simulation of the CDF detector and  $b$  tagging algorithm [19], the  $b$  meson species are tagged at a uniform rate, while the  $b$  baryons tagging efficiency is 80% of the meson efficiency [27]. This means that the effective mean lifetime of the  $b$  hadrons entering into our  $\langle L_{xy} \rangle$  estimate is higher than the average  $b$  hadron lifetime in Eq. 7 by an amount  $\Delta\tau = 0.007 \pm 0.002 \times 10^{-12}$ . This represents a  $0.40 \pm 0.1\%$  shift where the error takes into account the uncertainties in tagging and in the  $b$  baryon fraction, but does not include an uncertainty associated with the modeling of  $b$  baryon decays, for which there exists limited data at this time. For this reason we inflate our estimate by a factor of two, resulting in a 0.2% uncertainty in  $\langle L_{xy} \rangle$  resulting from the lower  $b$  tagging efficiency for  $b$  baryons. It is our expectation that Tevatron Run II studies of  $b$  baryons will permit a more rigorous treatment of this uncertainty.

### C. Uncertainties associated with Monte Carlo modeling of $t\bar{t}$ events.

There are a variety of uncertainties associated with the PYTHIA Monte Carlo modeling of  $t\bar{t}$  events that pertain to the production of jets. To ascertain the corresponding uncertainties in  $m_t$ , we follow the direct advice of the authors [28] or the current conventions of the CDF top quark mass group to vary control parameters involved in  $t\bar{t}$  event generation. The resulting datasets are then treated in the same manner as the default sample, and the resulting  $\langle L_{xy} \rangle$  values are used to extract values of  $m_t$  by means of the default mass estimator. The difference between the value obtained for each variation and that obtained with the default sample is then taken to be the corresponding systematic uncertainty.

The aspects of  $t\bar{t}$  event generation that could affect jet production rates, in order of appearance in the Monte Carlo generation process are:

1. Spin correlations.
2. Initial state radiation.
3. Final state radiation.
4. Interference of initial and final state radiation.
5. Multiple interactions.

Many of these are constrained by experimental results. Final state radiation in  $W \rightarrow q\bar{q}'$  decay, for instance, is equivalent to that in  $Z \rightarrow q\bar{q}$  decay which is very well understood from LEP I [29].

Spin correlations in PYTHIA are present for the  $b$  and the  $W$  decay products, but not for correlations between the two top quarks. In real experiments, there are also multiple interactions in beam-beam crossings. These phenomena are expected to have small effect on  $m_t$  results for this method and were not included in our studies.

Lowest order Feynman diagrams for initial and final state radiation from top quarks are shown in Fig. 6. To estimate the uncertainties associated with final state radiation we follow guidance provided by the authors of PYTHIA to the CDF top group [28] in regard to the variation of the scale,  $\Lambda_{QCD}$ , and the degree of interference with initial state radiation. For initial state radiation, this guidance is again applied to our LHC study, while for the

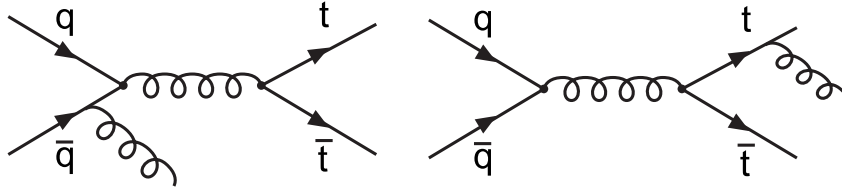


FIG. 6: Feynman diagrams for lowest order initial and final state radiation in  $t\bar{t}$  production. Interference between these processes is also taken into account. Final state radiation is also possible from the  $b$  quark and from the quarks appearing in hadronic decay of the  $W$ .

Tevatron, we use variations currently used by the CDF experiment that were determined by their studies of Drell-Yan di-muon events [30].

With regard to final state radiation, it is thought that PYTHIA may underestimate the gluon emission rate relative to the  $t\bar{t}$  + jet matrix elements at LHC energies [28] and so one might suspect, a priori, that the prescription used for the Tevatron could be inadequate for estimating LHC uncertainties. However, the event selection criteria that we use for the LHC, as presented below, is specifically chosen to suppress events with significant radiation. We therefore used the same parameter variations for final state radiation for both cases.

For all of our studies we use the CTEQ5 [31] parton density functions (PDFs) to create our default Monte Carlo event samples. To estimate the uncertainties associated with the PDFs, we generate  $t\bar{t}$  events using two variations of the MRS-98 [32] PDFs for which  $\Lambda_{QCD}$ , has values of 300 GeV and 229 GeV. The difference in final  $\langle L_{xy} \rangle$  values between the default CTEQ5 sample and the MRS-98 sample with  $\Lambda = 300$  GeV is added in quadrature with the difference in the two MRS-98 samples resulting from the variation of  $\Lambda_{QCD}$ . This procedure, while *ad hoc* in appearance, follows historical conventions at hadron colliders. Recently, however, a more sophisticated alternative has been suggested by the CTEQ collaboration [33] which we will apply in section IV.

To estimate an uncertainty on the modeling of the top quark  $p_T$  spectrum at the Tevatron, we took the tree-level spectrum obtained from PYTHIA and re-weighted the events to match the NNLO spectrum [34] at 1.96 TeV, normalized to equal area. We found the resultant shift in the extracted top quark mass to be  $0.9 \text{ GeV}/c^2$  for a generated mass of  $m_t = 178 \text{ GeV}/c^2$ . We draw several conclusions from this. First, for the purpose of our studies, the difference is small enough to justify our use of PYTHIA without inclusion of higher order ma-

trix elements. Second, the difference between the tree-level and NNLO spectra is expected to be significantly larger than the uncertainty on the NNLO calculation alone. Hence, in an actual measurement of  $m_t$ , one would avoid a significant uncertainty by using a Monte Carlo for which the top quark  $p_T$  spectrum is consistent with the NNLO prediction. Furthermore, at the LHC the  $t\bar{t}$  production rates are large enough to allow one to define an unbiased sample from which one could do a direct top quark  $p_T$  spectrum measurement. The Monte Carlo could be compared to measurement and tuned accordingly to allow the associated uncertainty in  $m_t$  to be reduced to a negligible level. We therefore do not assign an uncertainty associated with the top quark  $p_T$  spectrum in our studies.

### III. ESTIMATES BASED UPON CURRENTLY AVAILABLE INFORMATION.

As seen in Section II, many of the systematic uncertainties associated with this method are largely determined by the precision of experimentally determined quantities, such as the average  $b$  hadron lifetime. In this section we present estimates for the uncertainty on  $m_t$  for the Tevatron and the LHC using only information that is available at the present time. This has the virtue of yielding very sound estimates of systematic uncertainties. It does not, however, give a true picture of the precision that might be achieved with this method in the future, when much of the information that the method relies upon will be more refined than it is at present. This is particularly true in regard to the application of this method at the LHC where direct measurements with LHC  $t\bar{t}$  data will allow several of the larger systematic uncertainties to be reduced. This is discussed in Section IV below.

As mentioned in section I, the differences between the two environments lead to different event selection criteria. We focus on the lepton + jets event signature for the Tevatron, and dilepton event signature for the LHC, (see Fig. 7). In both cases, the term lepton actually refers to either a muon or electron from  $W$  decay and not a tau lepton, which is most often manifested experimentally as a narrow hadronic jet. Events in which the  $W$  decays leptonically tend to have smaller backgrounds, and hence dilepton event samples, in which both  $W$ 's decay leptonically, are the most pure. The all-hadronic  $t\bar{t}$  events are those for which both  $W$ 's decay to quarks. The dilepton, lepton+jets, and all-hadronic  $t\bar{t}$  events represent roughly 5%, 30%, and 45% of all  $t\bar{t}$  events, respectively.

At the Tevatron, where  $t\bar{t}$  yields are much smaller than at the LHC, the lepton+jets

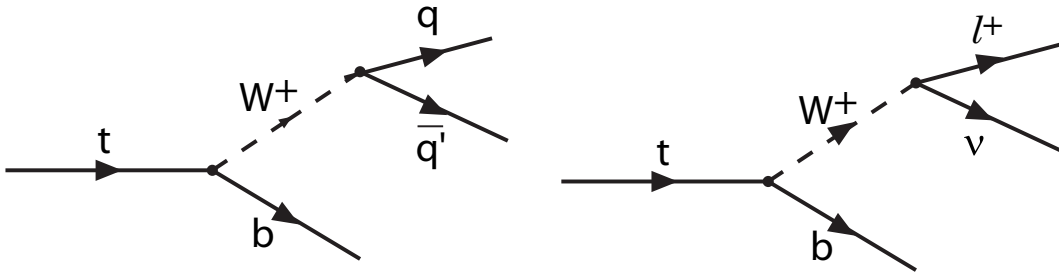


FIG. 7: The final state signatures for  $t\bar{t}$  events are determined by the  $W$ , which can decay either to quarks or to leptons. To determine  $m_t$  at the Tevatron, we studied the lepton + jets signature for  $t\bar{t}$  events in which one  $W$  decayed leptonically and the other hadronically. For the LHC we studied the dilepton signature for  $t\bar{t}$  in which the  $W$ 's decay to an electron or muon and their respective neutrino.

category provides the most significance. Our Tevatron study, therefore, is focused on this signature. We do, however, estimate the extent to which the uncertainty in  $m_t$  can be reduced by inclusion of dilepton events. For Tevatron event selection criteria, backgrounds contribute an uncertainty to  $m_t$  as a result of the uncertainties associated with both the normalization and shape of the  $L_{xy}$  distribution for each of the various background types.

At the LHC, it is more important to minimize systematic uncertainties. Thus, we focus on the dilepton signature to suppress backgrounds and reduce to minimize the occurrence of QCD radiation from final state partons. For the same purpose, we normalize our event counts to be consistent with the requirements that both  $b$  jets are tagged, and that there are no other jets in the event. As mentioned earlier, the “jet veto” also helps to minimize the probability that there is significant QCD radiation in the event.

### A. Estimates for the Fermilab Tevatron

Run II of the Tevatron is currently in progress. At the time of this writing, data from an integrated luminosity  $\sim 0.5 \text{ fb}^{-1}$  have been accumulated by each of the two collider experiments, CDF and D0. By the end of Run II it is expected that this will reach a value of 4.5 to  $8.5 \text{ fb}^{-1}$ .

As mentioned above, the use of the lepton+jets signature for  $t\bar{t}$  events is a compromise between sample purity and  $t\bar{t}$  event counts. Uncertainties associated with the modeling and normalizations of backgrounds contribute a Tevatron-specific uncertainty in  $m_t$ . We thus start with a discussion of our treatment of these backgrounds before summarizing all of our projected systematic and statistical uncertainties.

1. *Tevatron event selection.*

For our modeling of  $t\bar{t}$  events at the Tevatron, the tracks used to determine whether a given  $b$  or  $c$  hadron decay could produce an observable displaced vertex, as discussed in section II B 1, have impact parameter resolution comparable to that of the CDF experiment [19]. Thus, in Eq. 5, we use parameters:  $\alpha = 36 \mu\text{m}$  and  $\beta = 25 \mu\text{m-GeV}/c$ . Events are selected by requiring one lepton and one neutrino with transverse momentum of at least 20 GeV/ $c$ . There must be a total of 3 or more well-separated partons with transverse momenta of at least 15 GeV/ $c$ .

2. *Tevatron backgrounds.*

We considered various processes that can have similar characteristics to  $t\bar{t}$  events, and thus represent background constituents of Tevatron data sets. The relative proportion of any particular background type depends strongly on the event selection. We employ selection criteria used by the CDF collaboration for the lepton + jets signature [19], and therefore also assume the same types and relative proportions of backgrounds, with the exception of  $WW$ ,  $WZ$ ,  $ZZ$  and  $Z \rightarrow \tau\tau$  events which together represent only 2.3% of all backgrounds and so were ignored for simplicity. We thus consider the following final states:  $Wb\bar{b}$ ,  $Wc\bar{c}$ ,  $Wc$ ,  $b\bar{b}$  + jets, and mistags in  $W$ +jet events. Background sources are listed in Table II.

The contributions from single top quark production were also investigated. The t-channel production of a single top quark involves a rather different  $p_T$  spectrum than that found in  $t\bar{t}$  events and could therefore be treated as a “background”. However, it makes a negligible contribution after our event selection criteria are applied. The s-channel production of a single top quark has essentially the same dependence of  $\langle L_{xy} \rangle$  on  $m_t$  as that of  $t\bar{t}$  events and thus represents a potential signal source, but turns out to be negligible in comparison to the

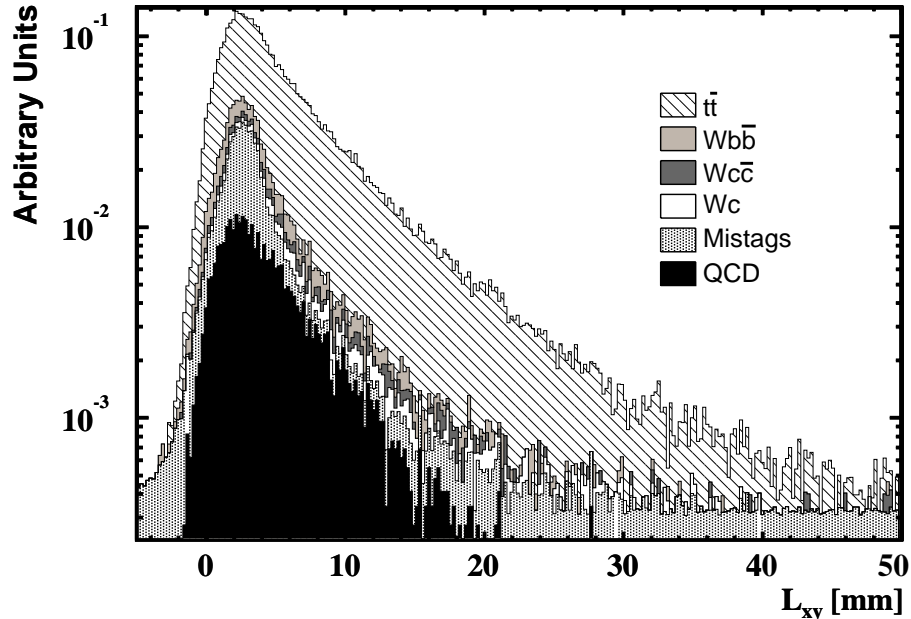


FIG. 8: The  $L_{xy}$  distribution for  $t\bar{t}$  with  $m_t = 175 \text{ GeV}/c^2$ , and the  $L_{xy}$  distributions for various backgrounds in lepton + jets events at the Tevatron. Default Monte Carlo parameters were used in addition to the parametric detector resolution model discussed in the text. The signal to background ratio is 3 to 1.

TABLE II: Various sources and proportions of backgrounds used in our studies, following ref. [19].

| Source                     | Fraction |
|----------------------------|----------|
| $Wb\bar{b}$                | 20.5%    |
| $Wc\bar{c}$                | 7.7%     |
| $Wc$                       | 8.9%     |
| $b\bar{b} + \text{jets}$   | 30.4%    |
| $W + \text{jets (mistag)}$ | 32.5%    |

contribution from  $t\bar{t}$ . For simplicity, we do not include either process in our studies.

Backgrounds were simulated using ALPGEN matrix elements [35], (including up to 2 additional radiated partons), together with the HERWIG parton shower model [15]. Each sample was processed with the same selection criteria as that applied to the  $t\bar{t}$  signal. For backgrounds involving charm, the  $c$  hadron daughter tracks were used for the tagging simulation,



and the kinematic cuts previously applied to  $b$  jets were applied to the  $c$  jets.

The signal for a given  $m_t$  was combined with the total background in a 3-to-1 ratio. The  $L_{xy}$  distributions for  $t\bar{t}$ , ( $m_t = 175 \text{ GeV}/c^2$ ), and backgrounds is seen in Fig. 8. The resulting values of  $\langle L_{xy} \rangle$  for the various  $m_t$  choices were then used to define a mass estimator for the Tevatron study.

### 3. Tevatron Results.

We determine the statistical uncertainty as described in section II for two different integrated luminosities at the Tevatron: the current value of  $500 \text{ pb}^{-1}$  and the maximum projected Run II value of  $8.5 \text{ fb}^{-1}$ . For each case, we estimate the corresponding numbers of top quarks and background events that we would expect to have by scaling results recently reported by CDF [19]. For top quark masses in the range  $130 \leq m_t \leq 230 \text{ GeV}/c^2$ , we create ensembles of large numbers of Monte Carlo samples as described in section II, and determine  $\langle L_{xy} \rangle$  for each. The mass estimator is then used to convert each value of  $\langle L_{xy} \rangle$  to a value of  $m_t$ . The distribution of “observed” values of  $m_t$  for a given ensemble has average value consistent with the mass value input to the Monte Carlo. From the distribution of observed  $m_t$  values for a given input mass and choice of integrated luminosity, we determine statistical uncertainties by constructing Neymann frequentist confidence intervals. Figures 9 and 10 show the results for integrated luminosities of  $500 \text{ pb}^{-1}$  and  $8.5 \text{ fb}^{-1}$ , respectively. In these figures, the dashed lines represent the confidence intervals used to determine statistical uncertainties. Thus, for instance, for a top quark mass of  $m_t = 178 \text{ GeV}/c^2$ , we expect that measurements done at the Tevatron will have statistical uncertainties of  $20.8 \text{ GeV}/c^2$  and  $5.0 \text{ GeV}/c^2$  for integrated luminosities of  $500 \text{ pb}^{-1}$  and  $8.5 \text{ fb}^{-1}$ , respectively.

The systematic uncertainties, obtained by the methods described in section II, are the same for both cases and are listed in Table III. The statistical uncertainty on the individual systematics listed in the table is  $\sim 0.2 \text{ GeV}/c^2$ .

To estimate the effect of adding  $t\bar{t}$  dilepton events, we scale event counts and tagged  $b$  jets based upon the results from a recent CDF  $t\bar{t}$  dilepton cross section measurement [36]. For an integrated luminosity of  $8.5 \text{ fb}^{-1}$  the statistical error is reduced from  $5.0$  to  $4.4 \text{ GeV}/c^2$ . For the most part, the systematic uncertainties associated with the dilepton signature will be similar to those for the lepton+jets signature, except for the uncertainty due to backgrounds

TABLE III: Systematic uncertainties for  $m_t = 175 \text{ GeV}/c^2$  for the Tevatron.

| Source                  | Uncertainty $\text{GeV}/c^2$ |
|-------------------------|------------------------------|
| Initial state radiation | 0.7                          |
| Final state radiation   | 1.1                          |
| Parton distributions    | 0.8                          |
| $b$ hadron lifetime     | 1.0                          |
| $b$ fragmentation       | 0.9                          |
| $b$ tagging             | 0.8                          |
| Backgrounds             | 0.3                          |
| Jet Energy Scale        | 1.9                          |
| TOTAL                   | 2.9                          |

which will be smaller.

### B. Estimates for the CERN LHC

For our LHC study, anticipated  $t\bar{t}$  production rates allow us to define event selection criteria that minimize uncertainties. We select only dilepton events in which the two leptons have transverse momenta of at least 35 and 25  $\text{GeV}/c$ . We also require two  $b$  jets with transverse energy above 15  $\text{GeV}/c$  and no other clustered energy above 10  $\text{GeV}$ . These event selection criteria effectively eliminate all backgrounds while minimizing the likelihood of QCD radiation. The effect of event selection on the transverse momenta of the top quarks is seen in Fig 11. For an integrated luminosity of  $10 \text{ fb}^{-1}$ , these requirements yield an expectation of  $\sim 13,000$  events, out of a  $\sim 8,000,000$  produced  $t\bar{t}$  events. It is estimated that these events have a ratio of  $t\bar{t}$  signal to backgrounds in excess of 30-to-1 [37]. We therefore do not include an uncertainty associated with backgrounds in our LHC study.

For our modeling of  $t\bar{t}$  events at the LHC, we use track impact parameter resolution parameters comparable to those of the CMS experiment [38]:  $\alpha = 15 \mu\text{m}$  and  $\beta = 75 \mu\text{m} - \text{GeV}/c$ .

We estimate a statistical uncertainty of  $0.9 \text{ GeV}/c^2$  for the LHC in  $10 \text{ fb}^{-1}$ , as seen in Fig 13. The systematic uncertainties are listed in Table IV. As for the Tevatron, the

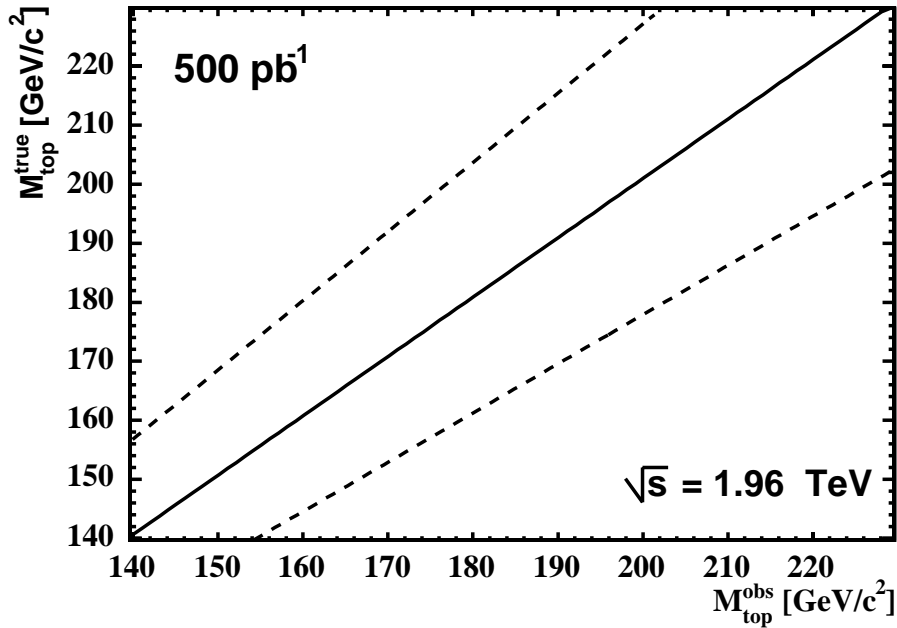


FIG. 9: The correlation of the input, (“true”), value of  $m_t$  with the measured, (“observed”), value of  $m_t$  (solid) is plotted for ensembles of Monte Carlo lepton + jets events for the Tevatron. The dashed lines are the one standard deviation contours (statistical only) for  $500 \text{ pb}^{-1}$  integrated luminosity. Default Monte Carlo parameters were used in addition to the parametric detector resolution model discussed in the text. The signal to background ratio is 3 to 1.

statistical uncertainty on the individual entries in the table is  $\sim 0.2 \text{ GeV}/c^2$ .

We did not include an uncertainty associated with  $b$  tagging efficiency. It is our expectation that the large  $t\bar{t}$  samples available at the LHC will allow the  $b$  tagging efficiency to be measured as a function of the summed  $p_T$  of the tracks, or the  $E_T$  of the  $b$  jet, with small uncertainty. To estimate the effect of the jet energy scale uncertainty, we varied jet energies by  $\pm 3\%$  in accordance with the CMS hadron calorimeter technical design report [39].

#### IV. FUTURE IMPROVEMENTS.

In the preceding sections we presented our estimates for the uncertainties on  $m_t$  using the mean decay length of  $b$  hadrons in  $t\bar{t}$  events at the Tevatron and LHC. We used only currently available information for modeling of  $t\bar{t}$  events. For the most optimistic Tevatron Run II integrated luminosity scenario, and using events with the lepton + jets signature,

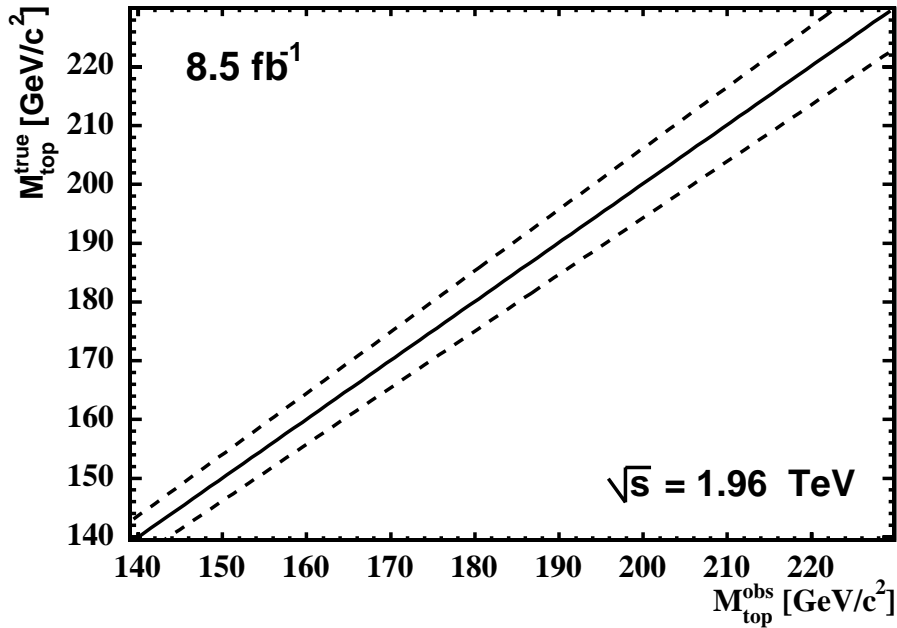


FIG. 10: The correlation of the input, (“true”), value of  $m_t$  with the measured, (“observed”), value of  $m_t$  (solid) is plotted for ensembles of Monte Carlo lepton + jets events for the Tevatron. The dashed lines are the one standard deviation contours (statistical only) for  $8.5 \text{ fb}^{-1}$  integrated luminosity. Default Monte Carlo parameters were used in addition to the parametric detector resolution model discussed in the text. The signal to background ratio is 3 to 1.

we obtained statistical and systematic uncertainties of  $5.0$  and  $2.9 \text{ GeV}/c^2$ , respectively. We estimated that the statistical uncertainty can be reduced to  $4.4 \text{ GeV}/c^2$  by inclusion of events conforming to the dilepton signature, without significantly affecting the systematic uncertainty. This corresponds to a total uncertainty of  $\sim 5 \text{ GeV}/c^2$ . Since our estimated statistical uncertainty is larger than our estimated systematic uncertainty, we do not expect this result to be improved without an increase in total integrated luminosity or an increase in the event identification or  $b$  tagging efficiencies. With regard to the former some small improvement could be obtained by loosening event selection criteria and allowing background to rise until an optimum total uncertainty is attained. With regard to  $b$  tagging, we have used currently achieved efficiencies, (in the range of 25-40%), that could turn out to be conservative. For instance, the CDF experiment has only recently begun to include information from the Layer 00 silicon detector [40, 41], which provides track hits at an average radius  $1.5 \text{ cm}$  that leads to a substantial improvement in track impact parameter resolution. The

TABLE IV: Systematic uncertainties for  $m_t = 175 \text{ GeV}/c^2$  for the LHC study.

| Source                  | Uncertainty $\text{GeV}/c^2$ |
|-------------------------|------------------------------|
| Initial state radiation | 1.3                          |
| Final state radiation   | 0.5                          |
| Parton distributions    | 0.7                          |
| $b$ hadron lifetime     | 1.3                          |
| $b$ fragmentation       | 1.2                          |
| Jet Energy Scale        | 0.2                          |
| TOTAL                   | 2.4                          |

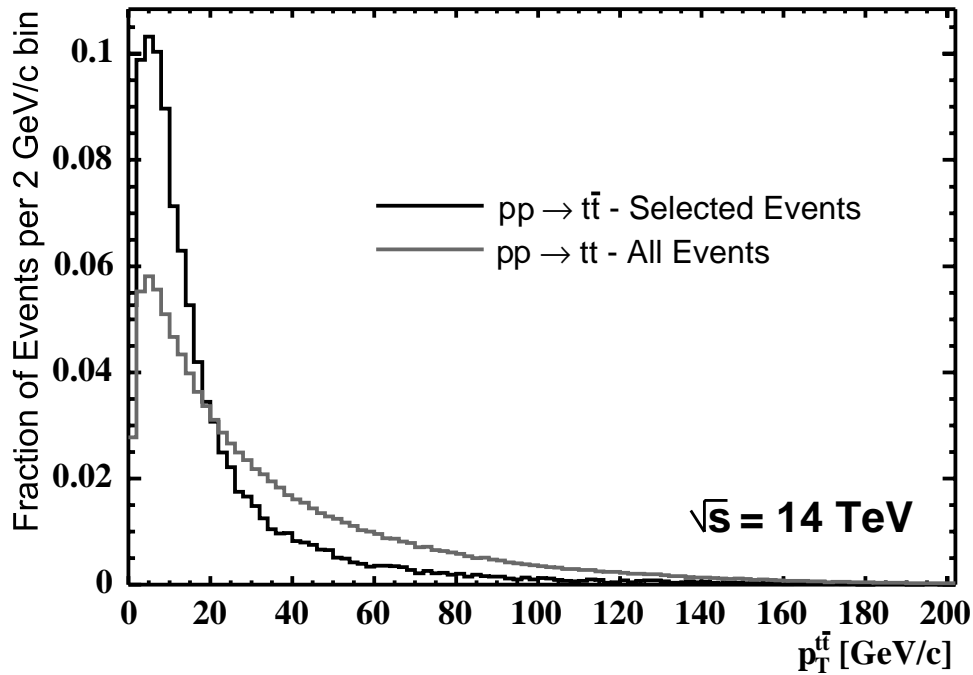


FIG. 11: The transverse momentum of the  $t\bar{t}$  pair at  $\sqrt{s} = 14 \text{ TeV}$  is plotted for all events, and for only those events passing the dilepton event selection discussed in the text. The curves are normalized to unit area.

D0 collaboration is now constructing a similar small radius silicon detector [42] to enhance their  $b$  tagging. These devices, as well as gradual improvements in the understanding and alignment of tracking detectors at the Tevatron will likely result in higher  $b$  tagging efficiencies. Thus, the actual statistical uncertainties on  $m_t$  per Tevatron experiment, for any

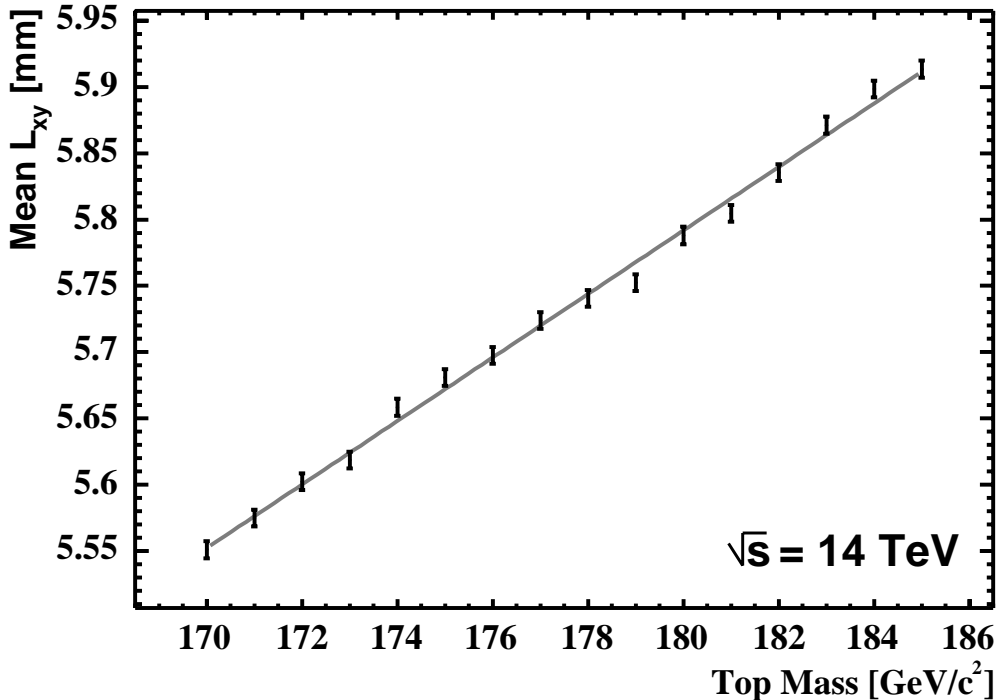


FIG. 12: An example of the correlation of  $L_{xy}$  with  $m_t$  for the default Monte Carlo and our particular choice of event selection criteria for the LHC. The correlation is well fit by a straight line over small mass ranges such as the one pictured here. Each point represents  $\sim 26,000$   $b$  jets in  $t\bar{t}$  events.

particular integrated luminosity, could be lower than the estimates presented above.

For  $10 \text{ fb}^{-1}$  integrated luminosity at the LHC, we projected statistical and systematic uncertainties of  $0.9$  and  $2.4 \text{ GeV}/c^2$ , respectively, corresponding to a total uncertainty of  $2.5 \text{ GeV}/c^2$ . Such precision is already significant, as it would allow for an important cross-check or improvement of other measurements of  $m_t$ . There is, however, the possibility for reduction of several of the systematic uncertainties associated with our LHC study.

As seen in Table IV, the dominant systematic uncertainties at the LHC are those associated with initial state radiation,  $b$  fragmentation, and the average  $b$  hadron lifetime. The uncertainty in the average  $b$  hadron lifetime, and lifetimes of the individual  $b$  hadron species, continue to improve with time and the accumulation of significantly larger  $b\bar{b}$  event samples at  $B$  factories and the Tevatron. It is therefore reasonable to anticipate that by the time this measurement is performed at the LHC, there will be a reduction in the uncertainties associated with the  $b$  lifetimes. The uncertainties associated with QCD radiation will be

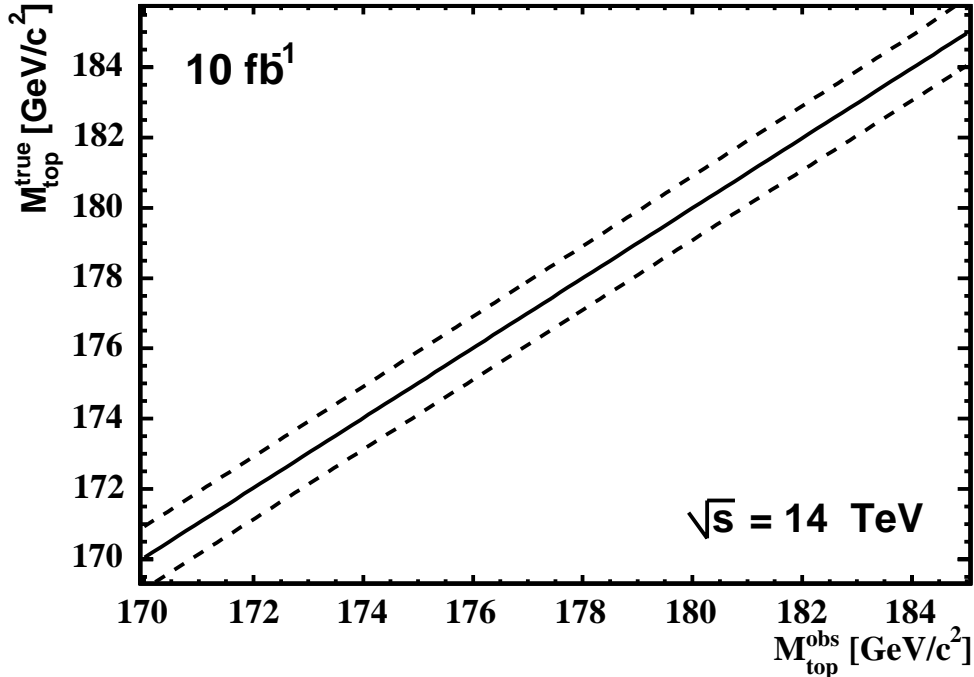


FIG. 13: The correlation of the input, (“true”), value of  $m_t$  with the measured, (“observed”), value of  $m_t$  (solid) is plotted for ensembles of Monte Carlo dilepton events for the LHC. The dashed lines are the one standard deviation contours (statistical only) for  $10 \text{ fb}^{-1}$  integrated luminosity.

significantly improved as a result of direct measurements at the Tevatron and LHC. Event samples containing millions of  $t\bar{t}$  events at the LHC will allow stringent constraints to be placed on the Monte Carlo modeling of QCD radiation that could reduce the corresponding systematic uncertainties to negligible levels. This in turn will allow event selection criteria to be loosened considerably to reduce the statistical uncertainty without significant penalty in the systematic uncertainty on  $m_t$ .

On the other hand, there are other systematic uncertainties that may not improve. For example, the average momentum carried by the  $b$  hadron in the process of fragmentation is an experimentally determined quantity that is currently dominated by the measurements with  $Z \rightarrow b\bar{b}$  events at LEP and SLD, which are limited by systematic uncertainties [16]. These measurements also benefited a great deal from the beam-energy constraint provided by collisions of electrons with positrons and are thus unlikely to be significantly improved at hadron colliders. It may, however, be possible for some overall improvement to be obtained by combining existing measurements.

With regard to parton distribution functions, it is difficult for us to say how much LHC data might improve the estimates we presented in Section III B, although some improvement seems inevitable. However, as we noted in Section II C, a more sophisticated algorithm PDF uncertainties has recently been developed. The CTEQ collaboration has established a new framework that enables correlations between the experimental measurements used to define the PDFs to be taken into account. It provides a pragmatic way to quantify uncertainties via an eigenvector approach to the Hessian method [33]. The eigenvectors form an orthonormal basis for a 20 dimensional parameter space of the 20 free parameters of the CTEQ6M fit. Forty-one PDF sets are generated, corresponding to positive and negative excursions along each of the 20 orthogonal axes in the parameter space, and the central CTEQ6M set. These can be used to estimate the uncertainty for any physical quantity that depends upon them, including the top quark mass, by adding in quadrature the differences between the positive and negative sets for each of the eigenvectors. When we apply this procedure to our Tevatron analysis, we obtain an uncertainty that is  $\sim 15\%$  smaller than our previous result shown in Table III.

These considerations lead us to conclude that by the time a measurement of the top quark mass has been performed at the LHC with  $10 \text{ fb}^{-1}$  of integrated luminosity, the result will be substantially more precise than the estimate we presented in section III B. For example, a factor of two reduction in the uncertainties associated with QCD radiation, together with smaller 10-40% reductions in the uncertainties associated with PDFs,  $b$  fragmentation, and average  $b$  hadron lifetime, reduce our total estimated uncertainty to  $\sim 1.5 \text{ GeV}/c^2$  per LHC experiment.

## V. CONCLUSION

We have presented a new method for the measurement of the top quark mass at the Tevatron and LHC that is largely uncorrelated with other methods. Initial studies using currently available information to model all aspects of  $t\bar{t}$  events yields uncertainties on  $m_t$  of  $\sim 5 \text{ GeV}/c^2$  for  $8.5 \text{ fb}^{-1}$  of integrated luminosity in Run II of the Tevatron and  $\sim 2.5 \text{ GeV}/c^2$  for  $10 \text{ fb}^{-1}$  of integrated luminosity at the LHC. Furthermore, with likely improvements in our understanding of  $b$  hadron properties and  $t\bar{t}$  events the uncertainties associated with this method at the LHC could be substantially reduced, making this method com-



parable in mass resolution to all other methods, for which a total uncertainty of 1.5-2.0 GeV/ $c^2$  per experiment is expected.

### Acknowledgments

We'd like to acknowledge the following people: D. Barge, C. Campagnari, F. Gianotti, D. Glenzinski, D. Rainwater, K. Smolek and U.K. Yang for insightful comments and contributions to this paper. This work was made possible by U.S. Department of Energy grant DE-FG03-91ER40618.

- 
- [1] D. Chakraborty, J. Konigsberg, and D. L. Rainwater, *Ann. Rev. Nucl. Part. Sci.* **53**, 301 (2003), hep-ph/0303092.
  - [2] C. Quigg, *Phys. Today* **50N5**, 20 (1997), hep-ph/9704332.
  - [3] W. J. Marciano (2004), hep-ph/0411179.
  - [4] Another quantity that does not suffer from jet energy scale uncertainty that we considered is the mean transverse energy of leptons from  $W$  decays in  $t\bar{t}$  events. Initial studies indicate that the correlation is too weak to be useful at the Tevatron, but could become important at the LHC. This was first suggested to us by C. Campagnari, The University of California Santa Barbara.
  - [5] J. Incandela, CDF note 1921, (1992).
  - [6] F. Abe et al. (CDF), *Phys. Rev. Lett.* **74**, 2626 (1995), hep-ex/9503002.
  - [7] S. Abachi et al. (D0), *Phys. Rev. Lett.* **74**, 2632 (1995), hep-ex/9503003.
  - [8] P. Azzi et al. (CDF Collaboration) (2004), hep-ex/0404010.
  - [9] V. M. Abazov et al. (D0), *Nature* **429**, 638 (2004), hep-ex/0406031.
  - [10] D. Amidei et al. (TeV-2000 Study Group) (1996), .SLAC-REPRINT-1996-085.
  - [11] R. Bonciani, S. Catani, M.L. Mangano and P. Nason, *Nucl. Phys. B* **529** 424 (1998), updated in arXiv:hep-ph/0303085.
  - [12] N. Kidonakis and R. Vogt, *Phys. Rev. D* **68**, 114014 (2003).
  - [13] I. Borjanovic et al. (2004), hep-ex/0403021.
  - [14] T. Sjostrand *et al.*, *Comp. Phys. Commun.* **135**, 238 (2001).

- [15] G. Marchesini *et al.*, *Comp. Phys. Commun.* **67**, 465 (1992); G. Corcell *et al.*, *J. High Energy Phys.* **01**, 010 (2001).
- [16] S. Eidelman *et al.* (Particle Data Group), *Phys. Lett.* **B592**, 1 (2004).
- [17] H. F. A. Group (2004), hep-ex/0412073.
- [18] We use a cylindrical coordinate system about the beam axis in which  $\theta$  is the polar angle,  $\phi$  is the azimuthal angle, and  $\eta \equiv -\ln \tan(\theta/2)$ .  $E_T \equiv E \sin \theta$  and  $p_T \equiv p \sin \theta$  where  $E$  is energy measured by the calorimeter and  $p$  is momentum measured by the spectrometer.  $\vec{E}_T \equiv -\sum_i E_T^i \mathbf{n}_i$ , where  $\mathbf{n}_i$  is the unit vector in the azimuthal plane that points from the beam line to the  $i$ th calorimeter tower.
- [19] D. Acosta *et al.* (CDF) (2004), hep-ex/0410041.
- [20] This was first suggested to us by M. Shochet, University of Chicago.
- [21] G. Abbiendi *et al.* (OPAL), *Eur. Phys. J.* **C29**, 463 (2003), hep-ex/0210031.
- [22] K. Abe *et al.* (SLD), *Phys. Rev.* **D65**, 092006 (2002), hep-ex/0202031.
- [23] A. Heister *et al.* (ALEPH), *Phys. Lett.* **B512**, 30 (2001), hep-ex/0106051.
- [24] DELPHI Collaboration, G. Barker *et al.*, DELPHI note: 2002-069-CONF-603 (2002).
- [25] G. Corcella (2004), hep-ph/0409120.
- [26] D. Abbaneo *et al.* (ALEPH) (2001), hep-ex/0112028.
- [27] D. Glenzinski, Fermilab, private communication.
- [28] T. Sjostrand, as presented to the CDF top group in 2004.
- [29] D. Y. Bardin *et al.* (1997), hep-ph/9709270.
- [30] U. K. Yang, The University of Chicago, private communication.
- [31] H. L. Lai *et al.* (CTEQ), *Eur. Phys. J.* **C12**, 375 (2000), hep-ph/9903282.
- [32] A. D. Martin, R. G. Roberts, W. J. Stirling, and R. S. Thorne, *Eur. Phys. J.* **C4**, 463 (1998), hep-ph/9803445.
- [33] J. Pumplin *et al.*, *JHEP* **07**, 012 (2002), hep-ph/0201195.
- [34] N. Kidonakis and R. Vogt (2004), hep-ph/0410367.
- [35] M. L. Mangano, M. Moretti, F. Piccinini, R. Pittau, and A. D. Polosa, *JHEP* **07**, 001 (2003), hep-ph/0206293.
- [36] D. Acosta *et al.* (CDF), *Phys. Rev. Lett.* **93**, 142001 (2004), hep-ex/0404036.
- [37] K. Smolek, ATLAS collaboration, private communication.
- [38] The CMS Collaboration, Addendum: CMS tracker TDR, CERN-LHCC-2000-016, (2000).

- [39] The CMS Collaboration, The hadron calorimeter TDR CERN-LHCC-97-31 (1997).
- [40] C. S. Hill (CDF), Nucl. Instrum. Meth. **A511**, 118 (2003).
- [41] T. K. Nelson (CDF), Int. J. Mod. Phys. **A16S1C**, 1091 (2001).
- [42] K. Hanagaki, Nucl. Instrum. Meth. **A511**, 121 (2003).